Asian Journal of Chemistry; Vol. 33, No. 7 (2021), 1663-1670

ASIAN JOURNAL OF CHEMISTRY

https://doi.org/10.14233/ajchem.2021.23286

Binding Constants Determination of Ofloxacin and Ornidazole Enantiomers with Sulfated β-Cyclodextrin as Single Ligand by Capillary Electrophoresis using Three Different Linear Plotting Methods

KHALDUN M. AL AZZAM

Pharmacological and Diagnostic Research Center (PDRC), Department of Pharmaceutical Sciences, Faculty of Pharmacy, Al-Ahliyya Amman University, Amman 19328, Jordan

Corresponding author: Tel: +962 796195880; E-mail: azzamkha@yahoo.com; k.azzam@ammanu.edu.jo

Received: 30 April 2021; *Accepted*: 31 May 2021; *Published online*: 26 June 2021; AJC-20411

The aim of this research is to use capillary electrophoresis to establish/determine the binding constants for ofloxacin and ornidazole enantiomers with the negatively charged chiral selector sulfated-β-cyclodextrin (S-β-CD). Using electrophoretic mobility values of ofloxacin and ornidazole enantiomers at various concentrations of S-β-CD used in the context of background electrolyte (BGE), binding constants were calculated using three separate linearization plots, namely double-reciprocal, X-reciprocal and Y-reciprocal. The R-ofloxacin enantiomer-S-β-CD complex had the highest inclusion affinity of the ofloxacin and ornidazole enantiomers, which matched with previously reported estimation. Every enantiomer-S-β-CD complex's binding constants, as well as thermodynamic binding parameters, were calculated at different temperatures. The host-guest binding constants using double reciprocal fit showed greater linearity ($R^2 > 0.99$) at all temperature ranges measured (15-30 ºC) as compared to the other two fit approaches. The thermodynamic complexation parameters were found to be dependent on the temperature of the enantiomers, as seen by the linear van't Hoff (15-30 ºC) plot.

Keywords: Binding constant, Enantiomers, Ofloxacin, Ornidazole, Sulfated-β-cyclodextrin.

INTRODUCTION

Ofloxacin is chemically known as (RS)-7-fluoro-2-methyl-6-(4-methylpiperazin-1-yl)-10-oxo-4-oxa-1-azatricyclo-[7.3.1.05,13]trideca-5(13),6,8,11-tetraene-11-carboxylic acid (Fig. 1). It is a fluoroquinolone that works against Gram-positive and Gram-negative bacteria both *in vivo* and *in vitro* [1-8]. With fluorinated quinolone [9], it is one of the most used antibiotics. The antibacterial efficacy of *levo*-enantiomer ofloxacin (S-(-) ofloxacin or levofloxacin) is 8-128 times that of *R*-(+)-ofloxacin and about two times that of the racemate, according to pharmacological studies [1,3,4,5,8]. Ofloxacin has two pK_a values one for carboxylic acid (pK_{a1} = 6.00) and another for the piperazine ring (pK_{a2} = 8.00) [10,11].

Ornidazole (Fig. 1) is chemically known as 1-chloro-3-(2-methyl-5-nitroimidazole-1-yl)propan-2-ol [12,13], with antiprotozoal and antibacterial properties [14,15]. It is used to cure anaerobic and microaerophilic bacteria and protozoa infections, as well as to prevent them. When given to pregnant women, ornidazole causes nausea, diarrhea, spermatotoxicity and extreme nervous system toxicity [15]. Ornidazole is also used in conjunction with fluoroquinolone to combat pelvic inflammatory disorders and infections [11,16]. Ornidazole has a single constant of ionization, with a pK_a of about 2.4 [13]. Past preclinical pharmacological studies have shown that the (+)-(*R*)-ornidazole toxicity is far greater than that of (-)-(*S*)-ornidazole.

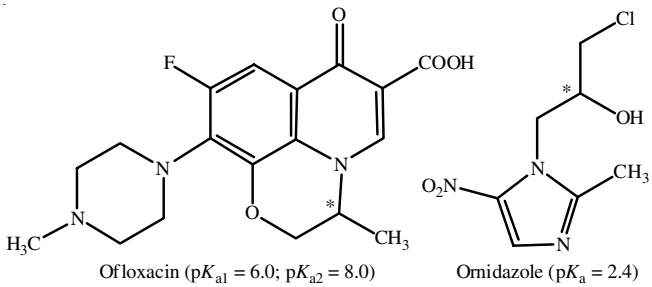

Ofloxacin (pK_{a1} = 6.0; pK_{a2} = 8.0) Ornidazole (pK_a = 2.4)

Fig. 1. The asterisks show the chiral center in the chemical structures of ofloxacin and ornidazole

Another study also showed that the removal of the enantiomers of ornidazole in beagle dogs was stereoselective [15]. Due to its high separation efficiency, low reagent consumption and rapid analysis times, capillary electrophoresis (CE) has been recognized as an effective enantioseparation technique [17-19]. In general, one of the enantiomer complexes with a chiral selector is preferred over the other, resulting in a dynamic equilibrium between the free analyte and the diastereomeric complex [17].

The use of CE to calculate binding constants is beneficial and appealing since the tests were carried out under identical enantioseparation conditions, with no changes or approximations. Binding constants as well as thermodynamic parameters measurements of host-guest complexes are important in many parts of study, including balancing dynamics, better understanding of molecular interactions, predicting migration behaviour and improving drug bioavailability [17,18,20,21].

Cyclodextrins (CDs) are extremely popular chiral selectors used in capillary electrophoresis (CE). Currently, a wide range of commercially available CDs are available, including native (α, β, γ) as well as neutral derivatives and charged [22]. On the other hand, sulfobutylated CD, sulfated CD and dextran sulfate are examples of negatively charged selectors that have been used widely in applications [23-25]. Furthermore, chiral selectors including the opposite charge to the analytes of interest have the benefit of counter-mobility, that allows for the utilization of minimal chiral selector concentrations [26].

Our group described using a single chiral selector with S-β-CD at the same run time to separate the enantiomers of ofloxacin and ornidazole [27]. Furthermore, theoretical simulations of enantiomeric inclusion complexes were carried out, rationalizing the reasons for the different migration actions of the four enantiomers of both ofloxacin and ornidazole. The purpose of this research is to further explain/expand on the host-guest complexes described previously by assessing the binding constants in addition thermodynamic parameters of the complexes [11]. Three linear plotting methods were used in the present study and the van't Hoff relationship was used to determine the thermo-dynamic that depend on temperature parameter. Additional thermodynamic parameters for instance complex electrophoretic mobility, isoenantioselective temperature and optimum cyclodextrin concentration for enantioseparation were determined as well.

EXPERIMENTAL

Ofloxacin, ornidazole, tris(hydroxymethyl)aminomethane and phosphoric acid (85%) were obtained from Sigma-Aldrich (St. Louis, USA). Sulfated-β-cyclodextrin (S-β-CD) (degree of sulfonate substitution ranged 7-11) was purchased from Aldrich (Milwaukee, USA). The Milli-Q device (Millipore, USA) provided deionized water, which was used to prepare of solutions.

Procedures: HP^{3D}CE capillary zone electrophoresis (CZE) system was used to perform the separations (Agilent Technologies, Germany). A photodiode array detector (DAD), equipped with the CZE, was used. Agilent Technologies provided a 50 μm i.d. 40 cm bare (uncoated) fused-silica capillary (detection length located, 8.5 cm away the capillary's outlet end). Uncoated fused silica capillaries are often used because they are cheaper than coated capillaries. As a data acquisition system, ChemStation software was used. After 30 min with 1 M NaOH, 10 min with 0.1 M NaOH and 15 min with water, the new capillary was conditioned. It was preconditioned with 0.1 M NaOH for 2 min between injections, then with water followed by BGE for another 2 min between runs. To avoid capillary surface adsorption, the capillary was flushed repeatedly for 15 min with 1 M NaOH and then for 20 min with BGE. The optimized electrophoretic conditions used in the current study were same as reported earlier [11], *i.e.* hydrodynamic injection at 50 mbar for 15 s was carried out using the following conditions: voltage, 18 kV at reversed polarity mode); capillary temperature, 25 ºC; detector wavelength, 230 nm; BGE compositions, 50 mM H_3PO_4/1.0 M tris solution, pH value 1.85; chiral selector concentration (S-β-CD), 30 mg mL^{-1} (12.19 mM). A 5 min wash with water was conducted by the end of the day. To make racemic ofloxacin and ornidazole standard solutions, a minimal volume of methanol was added to the required concentration (0.15 mM) and then topped up with water. A 0.20 μm membrane filter regenerated cellulose was used to filter all standard solutions, sample solutions, BGE and NaOH solutions. The temperature must be stabilized for not less than 5 min between each run to achieve repeatable results [28]. To correct mobility changes/shifts, methanol (0.5%, v/v) was used as an electroosmotic flow (EOF) marker [29]. Mobility was determined from the enantiomer and neutral migration times of the marker. Three times, both experiments have been performed. S-β-CD (0.5-28 mM) was used in the CE tests. The BGE viscosity at the same concentration of S-β-CD used in the CE experiments was measured using a Brookfield Viscometer instrument, model DV-II+ (Stoughton, USA).

Data evaluation

The following eqn. 1 was used to convert migration times (t) to mobility (μ_a) [30]:

$$\mu_a = \frac{I}{tE} = \frac{IL}{tV} \quad (1)$$

where $\mu_a = \mu_i + \mu_{EOF}$, V = applied voltage, I = detector's effective capillary length, L = total capillary length and E = electric field. The electrophoretic mobility and the electroosmotic mobility are defined by μ_i and μ_{EOF}, respectively.

RESULTS AND DISCUSSION

Binding constants determination: Understanding the behaviour of inclusion, such as supplying important data on the analyte-affinity in addition understanding molecular interactions, requires a thorough understanding of binding constants between the analyte and the chiral selector [20,30].

Wren & Rowe [31,32] established a theoretical model for studying the effect of CD concentration on mobility. Chiral discrimination is based on the difference in the enantiomer's free and complex electrophoretic mobility. The binding constant (K) can be estimated using the following equation [18]:

$$K[C] = \left(\frac{\mu_f - \mu_i}{\mu_i - \mu_c} \right) \quad (2)$$

where [C] is associated to the equilibrium concentration for the uncomplexed ligand, μ_f and μ_c are the electrophoretic mobilities parameters of both free and complexed analyte, respectively. μ_i is the analyte mobility at exact ligand concentration [C].

After complexing, the solvent must first undergo an electrophoretic mobility change. An analyte or ligand must be in the charged state under laboratory conditions investigated to meet such requirement. Additionally, the equilibrium timescale must be faster than the timescale for separation from the CE. The final measure is that both the free ligand and the ligand analyte complex must have adequate/sufficient concentrations [19,33, 34].

The linear plotting methods are the most effective approaches, where they weight data in correct/precise way [34]. Therefore, the double reciprocal, Y-reciprocal and X-reciprocal plotting methods were used to analyze the data for binding constants in the present research.

The double reciprocal method depends on the following equation:

$$\frac{1}{\mu_i-\mu_f}=\frac{1}{(\mu_i-\mu_f)K}\frac{1}{[C]}+\frac{1}{\mu_c-\mu_f} \quad (3)$$

A plot of $\frac{1}{\mu_i-\mu_f}$ *versus* $\frac{1}{[C]}$ gives, $K=\frac{\text{intercept}}{\text{slope}}$

The Y-reciprocal approach depends on the following equation:

$$\frac{[C]}{\mu_i-\mu_f}=\frac{1}{\mu_c-\mu_f}[C]+\frac{1}{(\mu_c-\mu_f)K} \quad (4)$$

A plot of $\frac{[C]}{\mu_i-\mu_f}$ *versus* [C] gives, $K=\frac{\text{slope}}{\text{intercept}}$

The X-reciprocal approach is based on the relationship:

$$\frac{\mu_i-\mu_f}{[C]}=-K(\mu_i-\mu_f)+K(\mu_i-\mu_f) \quad (5)$$

A plot of $\frac{\mu_i-\mu_f}{[C]}$ *versus* $(\mu_i-\mu_f)$ gives, K = –slope

The binding stiochiometry in the equations above is assumed to be 1:1. The linearity of the plots [35] confirms this statement. The mobilities of ofloxacin and ornidazole enantiomers were examined at diverse temperatures, where methanol was used as a neutral marker to compensate for EOF changes may occur.

The μ_{EOF} is reliant on the pH of the BGE. At low pH value, the EOF is likely to be insignificant (negligible), while at higher pH, it is likely to be significant [28]. Since, the EOF of a neutral marker will result in a non-zero effective mobility when it interacts with a charged complexing agent such as a chiral selector in the CE [36], the μ_{EOF} was calculated and computed using the neutral marker's migration time (Fig. 2) [28]. Methanol tends to be the most common EOF marker in articles examining the interaction constants of various analytes with charged cyclodextrins [36].

Furthermore, at pH = 2.50, the electroosmotic flow (EOF) is extremely low, resulting in extremely slow neutral marker mobility. When the capillary lengths, buffer solution composition and BGE ionic strength are all kept constant, the linear relationship between EOF mobility and current can be used as an alternative to calculate the EOF [37].

The first test was to see whether ofloxacin, ornidazole and chiral selector could be adsorbed to the capillary wall (due to a difference in the electrical double layer). Following several injections of analyte, the EOF variation was calculated using S-β-CD-free BGE. It was noted that the EOF remained constant over 23 successive introductions of an analyte to the CE system using the experimental part of the washing protocol. As a result, the capillary wall adsorption was shown to be insignificant. Besides as the BGE chiral selector (S-β-CD) in addition the silanol groups were protonated under the BGE conditions examined, chiral selector adsorption on the internal surface of the fused silica capillary was probable to be insignificant as well [33].

Capillary electrophoresis (CE) uses narrow bore fused silica capillaries with silanol groups on the inner wall. Because of the deprotonation of acidic silanol groups (pH values greater than 2.5), the inner surface of capillary becomes negatively charged. While using low pH buffers, the inner surface of silanols is not ionized; when using acidic pH, deprotonation of silanol groups at the fused silica inner surface is suppressed, resulting in a very low EOF. The use of a low pH of BGE inhibits charged CD adsorption by ensuring weak deprotonation of silanol groups at capillary walls [38].

S-β-CD concentration in BGE varied from 0.5 to 28 mm. As anticipated, adding S-β-CD to the BGE increases its viscosity and affecting electrophoretic mobilities. To fix the mobility changes triggered by the BGE properties, correction/normalization procedures are believed to be necessary (*e.g.* viscosity).

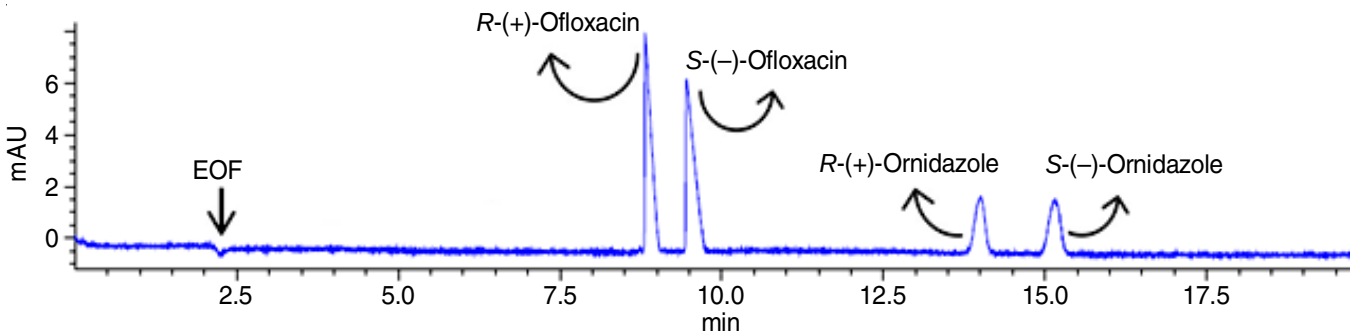

Fig. 2. Electropherograms generated by injecting racemic ofloxacin and ornidazole standards under the adopted CE conditions

The utilization of neutral additives' mobilities are corrected through multiplying the current ratio of each value in the presence and absence of additives. Current monitoring is therefore of importance, as charged additives can produce great current and hence lead to Joule heating [17,33].

The current formed in this study ranged from 13 A (without S-β-CD) to 49 μA (with the highest concentration of S-β-CD), corresponding to an electrical power of 882 mW and 1764 mW/m for a capillary length of 40 cm. This value (13 A) is insignificant since it is well below the generally accepted standard (thres-hold) of 5 W/m for 50 m i.d. capillary [29]. When no S-β-CD was utilized for viscosity, mobility was corrected by multi-plying each mobility value by the measured viscosity ratio at each concentration assessed.

Background electrolyte (BGE) viscosities varied from 1.11 (without S-β-CD) to 1.47 mm^2/s (28 mM S-β-CD) above the temperature tested over the range 15-30 ºC in the presence of changing amounts of S-β-CD (0.5-28 mM). At each concentration level of S-β-CD applied to BGE, the enantiomer mobilities were corrected for the EOF. The binding constants after corrections for both viscosity and EOF factors were calculated using the method described by Gratz & Stalcup [17] in eqn. 3 as follows:

$$\mu_{cor} = [(\mu_{obs}) - (\mu_{eof})]\left(\frac{\eta_o}{\eta_x}\right) \quad (6)$$

where μ_{cor}, μ_{obs} and μ_{eof} resemble the corrected electrophoretic mobility, observed electrophoretic mobility for analyte under experimental conditions and mobility of the neutral marker, respectively. η_x is the BGE viscosity at a given S-β-CD concentration, while η_o is the BGE viscosity without S-β-CD.

The ionic activity of BGE is affected by charged additives like S-β-CD, which may impair analyte mobility. The successful field strength felt/experienced by the analyte can be reduced by increasing the ionic strength (decrease its electrophoretic mobility). Additionally, when using uncoated fused silica capillaries, increased ionic strength causes a decrease in EOF (decreased zeta potential). Polyvalent species with high charged densities, such as S-β-CD, cannot contribute significantly to ionic strength, as their degree of substitution suggests.

Counterion condensation theory predicts that if the linear charged density of a covalent polyionic structure exceeds a critical value, a layer of condensed counterions will occur along the polyionic length, effectively reducing its linear charging density [17]. Since finding appropriate CD markers using linear plotting methods is challenging task, direct calculation of μ_c is considered impractical. However, accurate markers are only practicable for micellar systems and attaining saturated conditions needs μ_c to be measured using regression equations. The viscosity of BGE decreased and the frictional forces of complexed species decreased as the temperature increased [18,19].

Fig. 3(a-b) shows the disparity in mobility of ofloxacin and ornidazole enantiomers at various temperatures *versus* S-β-CD concentration. As the S-β-CD concentration increased, for the temperatures studied, the electrophoretic mobilities of ofloxacin and ornidazole enantiomers decreased. The maximum $\Delta_{\mu i}$ value between enantiomers occurs at the optimum concentration of CD $[C]_{opt}$ [18,39] and can be calculated using the Wren & Rowe model [31,32]:

$$[C]_{opt} = \frac{1}{\sqrt{K_S K_R}} \quad (7)$$

where K_S and K_R are the binding constants for the enantiomers S and R, respectively whether of ofloxacin or ornidazole enantiomers. The $[C]_{opt}$ values obtained (Tables 1 and 2) indicate that enantiomer has a high CD affinity, as seen in the complex of cyclodextrins and amino acid derivatives [39]. The mean $\Delta_{\mu i}$ values in all the experiments were smaller than the detected values.

Furthermore, the maximum experimental $\Delta_{\mu i}$ occurred at a lower concentration of S-β-CD than $[C]_{opt}$, which is associated with changes in viscosity when the BGE is added [18]. The maximum concentration was equivalent to the highest resolution. At the same concentration where $\Delta_{\mu i}$ is the largest, there will be no optimum resolution (data not shown). Other

TABLE-1
BINDING CONSTANT (M^{-1}) OBTAINED BETWEEN OFLOXACIN ENANTIOMERS UPON COMPLEXING WITH S-β-CD AT DIFFERENT TEMPERATURES

Temp. (°C)	Plotting method	K_S[a] (M^{-1})	K_R[a] (M^{-1})	α[b]	R^2 (*R*)	R^2 (*S*)	$[C]_{opt}$ (mM)
15	Double reciprocal	413.9	701.7	1.70	0.9957	0.9986	1.86
	X-reciprocal	467.9	762.1	1.63	0.9887	0.9915	1.67
	Y-reciprocal	420.3	585.7	1.39	0.9941	0.9918	2.01
17	Double reciprocal	415.5	697.7	1.68	0.9906	0.9967	1.86
	X-reciprocal	484.8	737.4	1.52	0.9504	0.9777	1.67
	Y-reciprocal	426.2	684.8	1.61	0.9809	0.9893	1.85
20	Double reciprocal	523.1	779.5	1.49	0.9921	0.9937	1.57
	X-reciprocal	411.2	678.6	1.65	0.9765	0.9604	1.89
	Y-reciprocal	424.4	732.9	1.73	0.9899	0.9729	1.79
25	Double reciprocal	518.0	649.5	1.25	0.9951	0.9915	1.72
	X-reciprocal	456.3	751.5	1.65	0.9802	0.9860	1.71
	Y-reciprocal	380.8	678.1	1.78	0.9810	0.9877	1.97
30	Double reciprocal	488.0	597.0	1.22	0.9931	0.9967	1.85
	X-reciprocal	464.6	635.1	1.37	0.9444	0.9727	1.84
	Y-reciprocal	408.1	659.3	1.62	0.9845	0.9788	1.93

[a]Binding constants for ofloxacin enantiomers; [b]Enantioselectivities of complexation; [c]Electrophoretic mobilities of enantiomer/S-β-CD complexes for ofloxacin enantiomers.

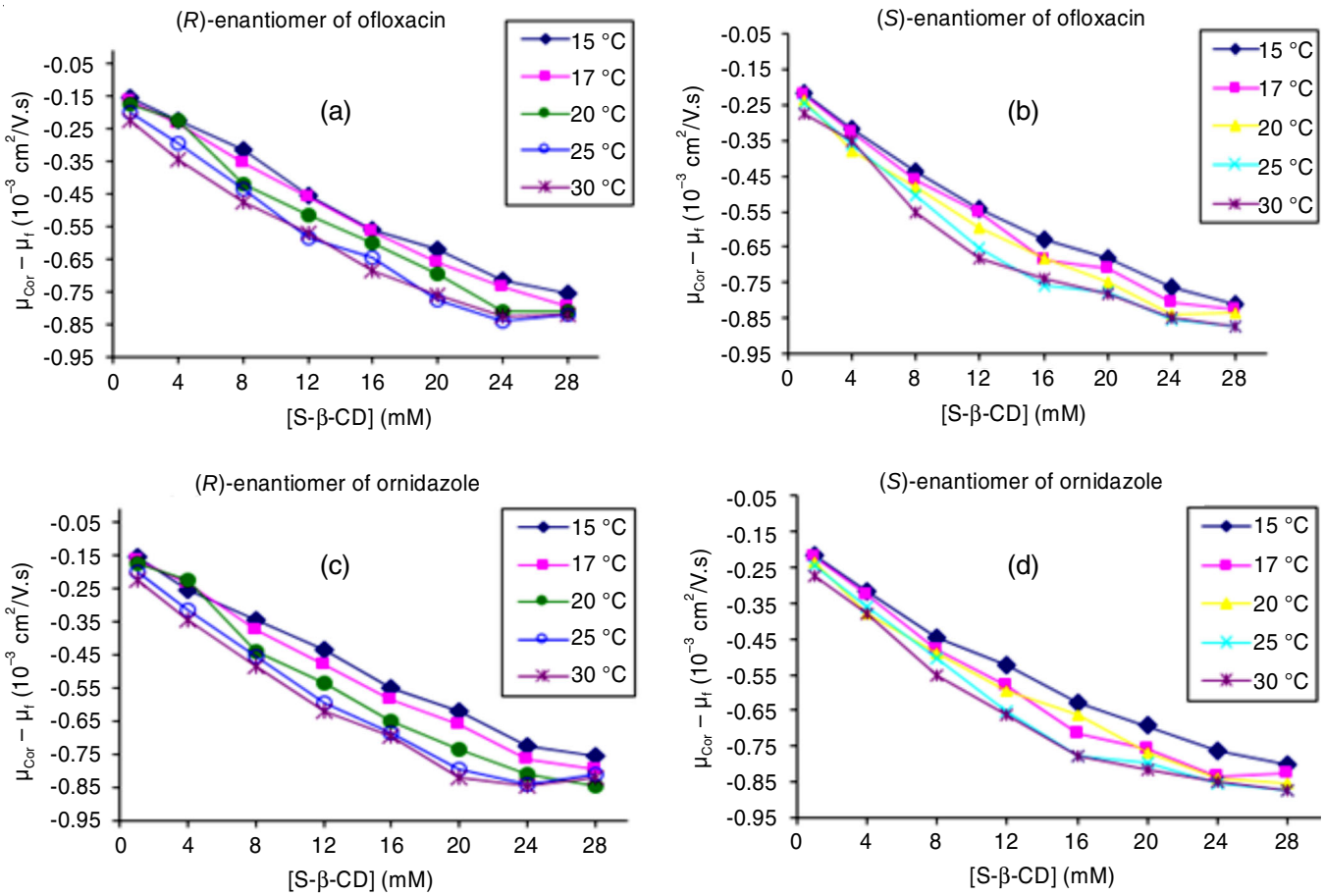

Fig. 3. Changes in the mobility of the enantiomers of ofloxacin (a & b) and ornidazole (c & d) *versus* S-β-CD concentration at various temperatures

TABLE-2
BINDING CONSTANT (M^{-1}) OBTAINED BETWEEN ORNIDAZOLE ENANTIOMERS UPON COMPLEXING WITH S-β-CD AT DIFFERENT TEMPERATURES

Temp. (°C)	Plotting method	K_R[a] (M^{-1})	K_S[a] (M^{-1})	α[b]	R^2 (*R*)	R^2 (*S*)	$[C]_{opt}$ (mM)
15	Double reciprocal	303.9	405.2	1.33	0.9934	0.9994	2.85
	X-reciprocal	319.9	420.1	1.31	0.9754	0.9902	2.73
	Y-reciprocal	306.2	398.7	1.30	0.9853	0.9921	2.86
17	Double reciprocal	300.7	380.5	1.27	0.9941	0.9907	2.96
	X-reciprocal	343.9	427.3	1.24	0.9702	0.9865	2.61
	Y-reciprocal	310.7	398.4	1.28	0.9872	0.9899	2.84
20	Double reciprocal	353.8	449.3	1.27	0.9947	0.9974	2.51
	X-reciprocal	299.2	387.3	1.29	0.9798	0.9805	2.94
	Y-reciprocal	330.8	410.0	1.24	0.9782	0.9847	2.72
25	Double reciprocal	385.9	480.5	1.25	0.9964	0.9910	2.32
	X-reciprocal	311.3	397.9	1.28	0.9868	0.9784	2.84
	Y-reciprocal	317.6	396.1	1.25	0.9892	0.9869	2.82
30	Double reciprocal	345.7	410.6	1.19	0.9925	0.9985	2.65
	X-reciprocal	359.4	448.0	1.25	0.9748	0.9865	2.49
	Y-reciprocal	322.6	398.3	1.23	0.9626	0.9767	2.79

[a]Binding constants for ornidazole enantiomers; [b]Enantioselectivities of complexation; [c]Electrophoretic mobilities of enantiomer/S-β-CD complexes for ornidazole enantiomers.

parameters like electroosmotic mobility, band broadening due to diffusion and other variables like injection and detector path length make resolution further tough [40]. Alternatively, some of the variations found may be due to measurement imprecision [18].

The binding constants between the enantiomers of ornidazole and ofloxacin with S-β-CD each and the results of enantioselectivity (α) at diverse temperatures and utilizing the three linear methods are shown in Tables 1 and 2. The binding constants were, as can be said, in the following order: R-ofloxacin enan-

tiomer-S-β-CD complex > S-ofloxacin enantiomer-S-β-CD complex > *R*-ornidazole enantiomer-S-β-CD complex > *S*-ornidazole enantiomer-S-β-CD complex, mean that (*R*)-enantiomer for both ofloxacin and ornidazole enantiomer has the greatest complexity.

It is already showed [11] that the inclusion complexes of S-β-CD with *S*- and *R*-ofloxacin enantiomers (-8853.29 and -8860.87 kJ mol^{-1}, respectively) have higher binding energies than their ornidazole counterparts (-8333.55 and -8336.55 kJ mol^{-1}, for S-β-CD with *S*- and *R*-ornidazole enantiomers, respectively). The S-β-CD will form more stable inclusion complexes with both the *S*- and *R*-enantiomers, owing to its high negative binding energies. The *R*-ornidazole/S-β-CD complex is somewhat more favourable than the S-ornidazole/S-β-CD complex with an energy difference of -7.76 kJ mol^{-1}. Ofloxacin enantiomers yielded similar findings. About this, difference in the *R*- and *S*-enantiomers' complexation energies is smaller (-4.28 kJ mol^{-1}). The energy gap between diastereoisomeric complexes, referred to as ΔE_{R-S} (-7.76 and -4.28 kJ mol^{-1} for ornidazole and ofloxacin enantiomers, respectively), is a metric of chiral separation that distinguishes the enantiomers and leads to the varying migration times found in laboratory studies. The negative values for ΔGº for both complexes mean that the guest molecule's attachment to the host is spontaneous, *i.e.* it's S-β-CD. The magnitude of the energy change reveals the driving force in the direction of complexity. Equilibrium favours the formation of complexes for both ofloxacin and ornidazole molecules, according to the results. The inclusion of one SO_4^{2-} group and the external part of the S-β-CD in the lowest energy conformation for ornidazole complexes showed a more favourable environment for recognition.

A close examination of ornidazole/S-β-CD complexes revealed that one of the sulfate groups formed hydrogen bonds with methyl H-atom as well as the chloropropyl groups in ornidazole (data not shown). The ornidazole enantiomers just provide a small interaction or contact with cyclodextrin's secondary rim and the sulfate group encapsulates rather than includes the guest molecule. A specific complexation activity was found in ofloxacin enantiomers. A piperazine ring fits closely and firmly into the center of the CD cavities, allowing the *R*-ofloxacin molecule to penetrate. The *S*-ofloxacin enantiomer's piperazine ring, on the other hand, is only partly included in the ring. It is observed that the sulfate group forms hydrogen bonds between the hydrogen atom of CH_2 in the oxazine ring and the oxygen atom in the sulfate group. Additionally, all *R*- and *S*-ofloxacin complexes showed coulombic bonding of CH···F forms. When complexed with ornidazole and ofloxacin molecules, the completely symmetrical CD host configuration becomes non-symmetrical. As the CD host configuration was complexed with ornidazole and ofloxacin molecules, the fully symmetrical structure became non-symmetrical. Since ornidazole is a smaller guest molecule than ofloxacin, it is expected to behave differently in terms of complexation and recognition. The central section of the CD cavity is unfavourable trapping region for ornidazole enantiomers, according to the potential energy profile of ornidazole/S-β-CD complexes. The stability of the inclusion complexes between the enantiomers and the CD allows for chiral separation, which leads to different migration times. Furthermore, these experiments have shown that stronger inclusion complexes lead to shorter elution times in reversed polarity CE runs [11]. The first, second, third and fourth electropherogram peaks can thus be attributed to *R*-ofloxacin, *S*-ofloxacin, *R*-ornidazole and *S*-ornidazole, respectively.

Enantioselectivity ($\alpha \geq 1.2$) has also been achieved. The double reciprocal plots achieved better linearity (as reflected by r^2) than the other plotting methods (Tables 1 and 2) since they can mask deviations from linearity at small ligand concentrations and were hence used for additional thermodynamic parameter measurements.

Thermodynamic parameters determination: Eqn. 8 [18,41] relates the equilibrium binding constant to the Gibbs free energy (ΔGº):

$$\Delta G^\circ = -RT \ln K \quad (8)$$

where R is the gas constant and T the absolute temperature.

The vant't Hoff isochore (eqn. 9) can be used to explain the temperature dependency of binding constants:

$$\ln K = -\frac{\Delta H^\circ}{RT} + \frac{\Delta S^\circ}{R} \quad (9)$$

Enthalpy change (ΔHº) is associated with complex formation and ΔSº the entropy changes. The energy of Gibbs, which relies on the enthalpy of the complex formation, shows a linear relationship in the van't Hoff plots. The temperature dependency of analyte partitioning from the aqueous phase to the pseudo-stationary phase, as well as entropy-controlled considerations, was suggested by non-linearity [18]. The ln α *vs.* 1/T van't Hoff plots for binding ofloxacin and ornidazole enantiomer-S-β-CD complexes are seen in Fig. 4(a-b).

Over the temperature range tested, linear relationships (r^2 = 0.9378 and 0.9190 for ofloxacin enantiomer-S-β-CD and ornidazole enantiomer-S-β-CD complexes, respectively) were obtained.

Since enantioselectivity depends on both the difference in enthalpy (ΔH°) and difference in entropy (ΔS°) of the inclusion interaction of the following eqn. 10 with increasing temperature, enantioselectivity decreased.

$$\ln \alpha = -\frac{\Delta\Delta H^\circ}{RT} + \frac{\Delta\Delta S^\circ}{R} \quad (10)$$

For ofloxacin and ornidazole enantiomers complexes, increases in enthalpies and entropies were observed to be (ΔHº = -2.183 and -0.5528 kJ mol^{-1}), (ΔS° = -7.044 and -1.645 J mol^{-1} K^{-1}), respectively. In the binding of ofloxacin and ornidazole enantiomers to S-β-CD, the negative values of ΔHº and negative values of ΔSº revealed that hydrogen bonding and van der Waals played a significant role [42]. For ofloxacin and ornidazole enantiomers complexes, the ΔG°_{298} values were -0.084 and -0.063 kJ mol^{-1}, respectively. The negative ΔGº indicates that complexation was favoured thermodynamically, proving that the binding mechanism is spontaneous [42]. The negative ΔSº indicates that entropy has unfavourable effect on ΔGº and as a result, on the separation process. At the same time, there are limitations in the degree of freedom of translation and rotating independence due to interaction between the host and

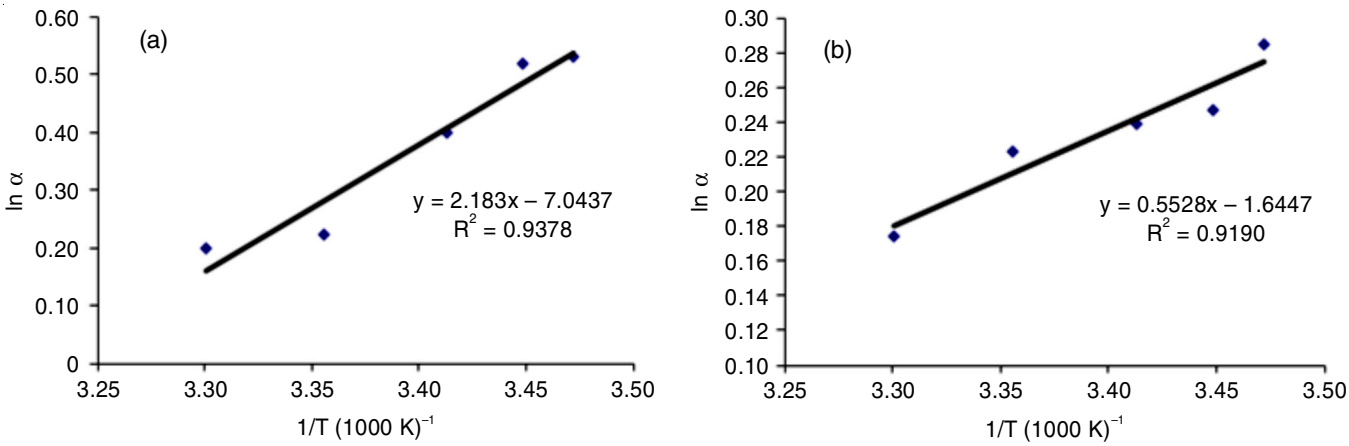

Fig. 4. Van't Hoff plots for (a) ofloxacin enantiomer/S-β-CD complexes and (b) ornidazole enantiomer/S-β-CD complexes

the guest, as well as variations in the composition and viscosity of the bulk material. Since these two opposing effects are normally balanced, entropy can only play a minor role in the forming of complexes [28,39,43].

The van't Hoff plots of chromatographic data (*i.e.* the logarithm of the retention or enantioseparation component *vs*. the inverse of the absolute temperature inverse) may be linear or non-linear, suggesting a particular retentive and selective process or a mixing mechanism for enantioseparation across the temperature range examined. As a result, thermodynamic study is a useful tool for investigating the role of chiral recognition. The isoenantioselective temperature (T_{iso}) can be calculated using the following eqn. 11 if the ΔH° and ΔS° quantities are known.

$$T_{iso} = \frac{\Delta\Delta H^\circ}{\Delta\Delta S^\circ} \quad (11)$$

Based on both eqns. 10 and 11, in all cases of enantioselective separations in which both the terms ΔS° and ΔH° are distinguished by an equal symbol, there is a temperature (T_{iso}) at which the enthalpy-entropy is compensated and the enantiomers coelute (*i.e.* α = 1) [44].

Entropy controls enantiomer separation at temperatures higher than T_{iso} ($|T\Delta S^\circ| > (|T\Delta H^\circ|$), while enthalpy controls enantiomer separation at temperatures lower than T_{iso} ($|T\Delta S^\circ| < (|T\Delta H^\circ|$) [44]. The existence of isoenantioselective temperature (T_{iso}) [45,46], *i.e.* temperature at which ΔG° is nil without enantiomers resolution, was indicated by the negative values obtained for both ΔH° and ΔS°. For ofloxacin and ornidazole enantiomers, the estimated T_{iso} are 36.9 and 63.0 °C, respectively. Above this temperature, the elution order of enantiomer will be inverted and eqn. 11 [18] can be used to describe it.

Cyclodextrins (CDs) may no more be a rigid cone, according to computational work, but are more likely to be a flexible, twisting basket that helps the guest molecule to fit. These dynamic properties are temperature-dependent and can increase the influence of complexation entropy to the energy of the molar Gibbs and thus the enantioselectivites [39].

Conclusion

The compliance of capillary electrophoresis (CE) technique is additional confirmed by the capability to use three linear plotting methods to estimate binding constants, namely double-reciprocal, *y*-reciprocal and *x*-reciprocal. The double-reciprocal solution proved to be more reliable between the three fits. In addition, related thermodynamic parameters have also been achieved. The results showed that the binding constants were in the following order: *R*-ofloxacin enantiomer-S-β-CD complex > *S*-ofloxacin enantiomer-S-β-CD complex > *R*-ornidazole enantiomer-S-β-CD complex > S-ornidazole enantiomer-S-β-CD complex, indicating a greater complexity of (*R*)-enantiomer for each ofloxacin and ornidazole enantiomers. Intrinsic CE features for instance high performance, high resolution capacity, small sample consumption and fast analysis time make the identification of binding constants useful. Furthermore, the additional benefit of the use of CE compared to HPLC is the small number of guests and hosts needed for the determination of binding constants.

CONFLICT OF INTEREST

The authors declare that there is no conflict of interests regarding the publication of this article.

REFERENCES

1. B. Awadallah, P.C. Schmidt and M.A. Wahl, *J. Chromatogr. A*, **988**, 135 (2003); https://doi.org/10.1016/S0021-9673(02)02015-0
2. B. Li, Z. Zhang, L. Zaho and C. Xu, *Talanta*, **57**, 765 (2002); https://doi.org/10.1016/S0039-9140(02)00093-0
3. M.A. Garcia, C. Solans, A. Calvo, M. Royo, E. Hernandez, R. Rey and M.A. Bregante, *Chromatographia*, **56**, 39 (2002); https://doi.org/10.1007/BF02490244
4. C. Horstkötter and G. Blaschke, *J. Chromatogr. B Biomed. Sci. Appl.*, **754**, 169 (2001); https://doi.org/10.1016/S0378-4347(00)00595-8
5. T. De Boer, R. Mol, R.A. de Zeeuw, G.J. de Jong and K. Ensing, *Electrophoresis*, **22**, 1413 (2001); https://doi.org/10.1002/1522-2683(200105)22:7<1413::AID-ELPS1413>3.0.CO;2-U.
6. O. Ballesteros, J.L. Vílchez and A. Navalón, *J. Pharm. Biomed. Anal.*, **30**, 1103 (2002); https://doi.org/10.1016/S0731-7085(02)00466-1
7. L. da Silveira Ev and E.E.S. Schapoval, *J. Pharm. Biomed. Anal.*, **27**, 91 (2002); https://doi.org/10.1016/S0731-7085(01)00513-1
8. T. Arai and H. Kuroda, *Chromatographia*, **32**, 56 (1991); https://doi.org/10.1007/BF02262467

9. G.-W. Cheng, H.-L. Wu and Y.-L. Huang, *Anal. Chim. Acta*, **616**, 230 (2008); https://doi.org/10.1016/j.aca.2008.04.012
10. J. Barbosa, R. Bergës and V. Sanz-Nebot, *J. Chromatogr. A*, **823**, 411 (1998); https://doi.org/10.1016/S0021-9673(98)00428-2
11. K.M. Al Azzam, B. Saad, R. Adnan and H.Y. Aboul-Enein, *Anal. Chim. Acta*, **674**, 249 (2010); https://doi.org/10.1016/j.aca.2010.06.046
12. M.-H. Wang, Z.-C. Tan, X.-H. Sun, F. Xu, Y.-F. Liu, L.-X. Sun and T. Zhang, *Thermochim. Acta*, **414**, 25 (2004); https://doi.org/10.1016/j.tca.2003.11.005
13. K.L. See, A.A. Elbashir, B. Saad, A.S.M. Ali and H.Y. Aboul-Enein, *Biomed. Chromatogr.*, **23**, 1283 (2009); https://doi.org/10.1002/bmc.1251
14. L. Zhang, Z. Zhang and K. Wu, *J. Pharm. Biomed. Anal.*, **41**, 1453 (2006); https://doi.org/10.1016/j.jpba.2006.03.016
15. H. Wang, Y. Chen, J. Zhou, C. Ma, Y. Chen and X. Liu, *Chromatographia*, **67**, 875 (2008); https://doi.org/10.1365/s10337-008-0625-3
16. B.N. Suhagia, S.A. Shah, I.S. Rathod, M.H. Patel, D.R. Shah and B.P. Marolia, *Anal. Sci.*, **22**, 743 (2006); https://doi.org/10.2116/analsci.22.743
17. S.R. Gratz and A.M. Stalcup, *Anal. Chem.*, **70**, 5166 (1998); https://doi.org/10.1021/ac980780i
18. N. Pang, Z. Zhang, Y. Bai and H. Liu, *Anal. Bioanal. Chem.*, **393**, 313 (2009); https://doi.org/10.1007/s00216-008-2446-5
19. K.L. Rundlett and D.W. Armstrong, *Electrophoresis*, **18**, 2194 (1997); https://doi.org/10.1002/elps.1150181210
20. Z. Chen and S.G. Weber, *Trends Analyt. Chem.*, **27**, 738 (2008); https://doi.org/10.1016/j.trac.2008.06.008
21. J. Tellinghuisen, *Biophys. Chem.*, **120**, 114 (2006); https://doi.org/10.1016/j.bpc.2005.10.012
22. H. Nishi and S. Terabe, *J. Chromatogr. A*, **694**, 245 (1995); https://doi.org/10.1016/0021-9673(94)00682-Y
23. R.J. Tait, D.O. Thompson, V.J. Stella and J.F. Stobaugh, *Anal. Chem.*, **66**, 4013 (1994); https://doi.org/10.1021/ac00094a025
24. A.M. Stalcup and K.H. Gahm, *Anal. Chem.*, **68**, 1360 (1996); https://doi.org/10.1021/ac950764a
25. K.-H. Gahm and A.M. Stalcup, *Chirality*, **8**, 316 (1996); https://doi.org/10.1002/(SICI)1520-636X(1996)8:4<316::AID-CHIR5>3.0.CO;2-D
26. G. Subramanian, Chiral Separation Techniques, Wiley: Weinheim, Eds. 3 (2007).
27. K.M. Al Azzam, B. Saad, R. Adnan and M.I. Saleh, *Mikrochim. Acta*, **166**, 311 (2009); https://doi.org/10.1007/s00604-009-0209-4
28. C. Danel, N. Azaroual, A. Brunel, D. Lannoy, G. Vermeersch, P. Odou and C. Vaccher, *J. Chromatogr. A*, **1215**, 185 (2008); https://doi.org/10.1016/j.chroma.2008.10.094
29. D. El-Hady, S. Kühne, N. El-Maali and H. Wätzig, *J. Pharm. Biomed. Anal.*, **52**, 232 (2010); https://doi.org/10.1016/j.jpba.2009.12.022
30. Y. Shakalisava and F. Regan, *Electrophoresis*, **27**, 3048 (2006); https://doi.org/10.1002/elps.200500842
31. S.A.C. Wren and R.C. Rowe, *J. Chromatogr. A*, **603**, 235 (1992); https://doi.org/10.1016/0021-9673(92)85366-2
32. S.A.C. Wren and R.C. Rowe, *J. Chromatogr. A*, **609**, 363 (1992); https://doi.org/10.1016/0021-9673(92)80181-S
33. C. Karakasyan, M. Taverna and M.-C. Millot, *J. Chromatogr. A*, **1032**, 159 (2004); https://doi.org/10.1016/j.chroma.2003.11.021
34. M.S. Bellini, Z. Deyl, G. Manetto and M. Kohlíèková, *J. Chromatogr. B Biomed. Sci. Appl.*, **924**, 483 (2001); https://doi.org/10.1016/S0021-9673(01)00775-0
35. Y. Tanaka and S. Terabe, *J. Chromatogr. B Analyt. Technol. Biomed. Life Sci.*, **768**, 81 (2002); https://doi.org/10.1016/S0378-4347(01)00488-1
36. L. Müllerová, P. Dubski, J. Svobodová and B. Gaš, *Electrophoresis*, **34**, 768 (2013); https://doi.org/10.1002/elps.201200490
37. C. Lancioni, S. Keunchkarian, C.B. Castells and L.G. Gagliard, *Talanta*, **192**, 448 (2019); https://doi.org/10.1016/j.talanta.2018.09.044
38. G. Gübitz and M.G. Schmid, Chiral Separations Methods and Protocols, Humana Press Inc.: Totowa, NJ (2004).
39. A. Van Eeckhaut, S. Boonkerd, M.R. Detaevernier and Y. Michotte, *J. Chromatogr. A*, **903**, 245 (2000); https://doi.org/10.1016/S0021-9673(00)00897-9
40. W. Lindner, B. Böhs and V. Seidel, *J. Chromatogr. A*, **697**, 549 (1995); https://doi.org/10.1016/0021-9673(94)01240-F
41. Y.S. Ding, B.C. Lin and C.W. Huie, *Chromatographia*, **52**, 367 (2000); https://doi.org/10.1007/BF02491034
42. B. Liu, C. Xue, J. Wang, C. Yang and Y. Lv, *Biochem. Indian J.*, **5**, 229 (2011).
43. R. Kuhn, F. Erni, T. Bereuter and J. Haeusler, *Anal. Chem.*, **64**, 2815 (1992); https://doi.org/10.1021/ac00046a026
44. C. Panella, R. Ferretti, A. Casulli and R. Cirilli, *J. Pharm. Anal.*, **9**, 324 (2019); https://doi.org/10.1016/j.jpha.2019.04.002
45. A. Berthod, W. Li and D.W. Armstrong, *Anal. Chem.*, **64**, 873 (1992); https://doi.org/10.1021/ac00032a009
46. C. Danel, E. Lipka, J.-P. Bonte, J.-F. Goossens, C. Vaccher and C. Foulon, *Electrophoresis*, **26**, 3824 (2005); https://doi.org/10.1002/elps.200500078